

## Measurements-induced dynamics of a micromaser

P. Meystre and E. M. Wright

*Optical Sciences Center, University of Arizona, Tucson, Arizona 85721*

(Received 6 July 1987)

Repeated measurements of the atomic inversion are incorporated in the theory of the micromaser. Two examples of measurements-induced dynamics are presented which display (a) quantum diffusion above a potential barrier and (b) an instability in the form of quantum-mechanical relaxation oscillations. Implications of these results on the study of the quantum-classical interface are briefly discussed.

### I. INTRODUCTION

It has been pointed out by Lamb that in order to study the dynamical behavior of a quantum system, it is necessary to explicitly include the effects of the measurements that must be performed in order to monitor it. To properly do so requires coupling the system under investigation to a meter system. The measurement process typically produces a back action on the system which influences its future dynamics. This is quite different from the classical situation, where "any observation of the system would involve some intervention from outside the system, but the structure of the theory is such that the effects of measurements can easily be ignored."<sup>1</sup>

In this paper we analyze the influence of repeated measurements on a micromaser.<sup>2</sup> They lead to measurements-induced dynamics and instabilities which are not apparent when conventional ensemble average predictions are considered, i.e., when the system is prepared to a fresh initial state after each measurement, wiping out any memory of the past in the process.

In a micromaser, a low-density beam of two-level (Rydberg) atoms is passed through a single-mode, high- $Q$  microwave cavity at such a low rate that at most one atom at a time is present inside the cavity. Because there is no efficient photon detector in the microwave regime, the atoms play a dual role of both pumps and detectors. Monitoring the state of the two-level atoms as they exit the cavity, e.g., by the technique of field ionization, is used to extract information about the cavity mode. If the state of the atoms is not measured as they exit the cavity the field density matrix always evolves towards a unique steady state.<sup>3</sup> In contrast, we show in this paper that if the state of the exiting atoms is monitored the density matrix evolves in time and the system exhibits dynamics and instabilities for arbitrarily long times (as opposed to transients).

This paper is organized as follows. Section II reviews the theoretical model of the micromaser and discusses the way in which we determine representative outcomes of repeated measurements on the system. Section III illustrates this procedure for the situation where the effective potential<sup>3</sup> of the micromaser exhibits two minima of equal depth. In this case, repeated measurements lead to quantum diffusion above the potential barrier between

the two corresponding values of the intracavity intensity. Section IV considers the situation where the vacuum field is seen by the atoms flying through the cavity as a  $2n\pi$ -pulse,  $n$  integer. Under these conditions, thermal fluctuations lead to measurements-induced instabilities in the form of quantum-mechanical relaxation oscillations. Finally, Sec. V is a summary and conclusion.

### II. MICROMASER WITH REPEATED MEASUREMENTS

#### A. Conventional approach

We consider a micromaser consisting of a single-mode microwave cavity of extremely high quality factor,  $Q \cong 10^{11}$ , in which two-level atoms are injected at such a low rate  $R$  that at most one atom at a time is present inside the resonator.<sup>2</sup> Due to the combined effects of the high- $Q$  factor and the large dipole moment  $\kappa$  of the Rydberg atoms used in the experiments, the maser threshold is reached for values of  $R$  such that the probability for an atom to be inside the cavity at a given time is considerably less than 1. Also, the cavity damping is so weak that it is a good approximation to neglect dissipation when an atom is present inside the cavity.<sup>4,3</sup> Under these conditions, the atom-field interaction can be simply described by the Jaynes-Cummings Hamiltonian<sup>5</sup>

$$\mathcal{H} = (\hbar\omega/2)S_3 + \hbar\omega a^\dagger a + \hbar\kappa/2(S_+ a + a^\dagger S_-), \quad (1)$$

where  $S_3$ ,  $S_+$ , and  $S_-$  are spin operators,  $a$  and  $a^\dagger$  the field annihilation and creation operators,  $[a, a^\dagger] = 1$ , and we consider for simplicity exact resonance between the cavity mode and atomic transition frequencies  $\omega$ . When atom  $i$  leaves the resonator, the atom-field system is left in the state described by the density matrix

$$\rho(t_i + t_{\text{int}}) = U(t_{\text{int}})\rho(t_i)U^\dagger(t_{\text{int}}), \quad (2)$$

where  $U(t) = \exp(-i\mathcal{H}t/\hbar)$ ,  $\rho(t_i)$  is the atom-field density matrix at the time  $t_i$  of injection of atom  $i$  and  $t_{\text{int}}$  its time of flight through the cavity. For simplicity, we consider a monoenergetic atomic beam so that  $t_{\text{int}}$  is independent of  $i$ .

If no measurement is performed on the state of the atom, the reduced density matrix  $\rho_f$  for the field just after atom  $i$  is found to exit the cavity is

$$\rho_f(t_i + t_{\text{int}}) = \text{Tr}_A [U(t_{\text{int}})\rho(t_i)U^\dagger(t_{\text{int}})], \quad (3)$$

where  $\text{Tr}_A$  denotes trace over the atomic states. The corresponding photon statistics  $p_n = \langle n | \rho_f | n \rangle$  is<sup>3</sup>

$$p_n(t_i + t_{\text{int}}) = p_{n-1}(t_i) \sin^2 \frac{1}{2} \Omega_n t_{\text{int}} + p_n(t_i) \cos^2 \frac{1}{2} \Omega_{n+1} t_{\text{int}}, \quad (4)$$

where  $\Omega_n = \kappa \sqrt{n}$  is the resonant “ $n$ -photon” Rabi frequency and  $p_n(t_i)$  is the field photon statistics just before injection of atom  $i$ .

In the interval  $t_p \cong 1/R$  between  $t_i + t_{\text{int}}$  and  $t_{i+1}$  when the next atom enters the cavity, the field density matrix evolves according to the standard master equation for a damped harmonic oscillator, which reads in component form

$$\dot{p}_n = \gamma(n_b + 1)[(n+1)p_{n+1} - np_n] + \gamma n_b [np_{n-1} - (n+1)p_n]. \quad (5)$$

Here  $n_b$  is the average number of thermal quanta in the reservoir and  $\gamma = \omega/Q$  is the cavity damping rate. Successive iterations of this procedure eventually lead to a steady-state regime. Assuming that the atoms are injected inside the cavity in their excited state  $|a\rangle$  and that the field is initially in thermal equilibrium,

$$p_n(0) = \frac{1}{1+n_b} \left[ \frac{n_b}{1+n_b} \right]^n \quad (6)$$

yields the steady-state photon statistics<sup>3</sup>

$$p_n = C \left[ \frac{n_b}{1+n_b} \right]^n \prod_{k=1}^n \left[ 1 + \frac{N_{\text{ex}}}{n_b} \frac{\sin^2(\Omega_k t_{\text{int}}/2)}{k} \right], \quad (7)$$

where

$$N_{\text{ex}} = R/\gamma \quad (8)$$

is the average number of atoms that traverse the cavity per damping time.

### B. Repeated measurements

The theory of Sec. II A implicitly assumes that the atoms are detected as they exit the resonator, as evidenced by the trace in Eq. (3). If that were not this case, we would not be justified in reducing the Hilbert space of the total system to that of the cavity mode only after each iteration. However, we did not ask specifically for the state of the exiting atom. We now show how to proceed in this case, and demonstrate that such measurements lead to totally different dynamics of the micromaser.

We assume for simplicity that the state of the atom is determined just after it exits the cavity. After the measurement, the field density matrix reduces to<sup>6,7</sup>

$$\rho_f(t_i + t_{\text{int}}) = \text{Tr}_A [ |s\rangle \langle s| U(t_{\text{int}})\rho(t_i)U^\dagger(t_{\text{int}}) ], \quad (9)$$

and the corresponding photon statistics are

$$p_n^a(t_i + t_{\text{int}}) = \mathcal{N}_a p_n(t_i) \cos^2 \frac{1}{2} \Omega_{n+1} t_{\text{int}}, \quad (10a)$$

or

$$p_n^b(t_i + t_{\text{int}}) = \mathcal{N}_b p_{n-1}(t_i) \sin^2 \frac{1}{2} \Omega_n t_{\text{int}}, \quad (10b)$$

depending upon whether the atom is found in the state  $s = |a\rangle$  or  $|b\rangle$ . The constants  $\mathcal{N}_a$  and  $\mathcal{N}_b$  guarantee that the field density matrix remains normalized after the measurement.

To obtain a specific realization of a sequence of such measurements we note that the probability for atom  $i$  to exit the cavity in its upper state is

$$p_a(t_i + t_{\text{int}}) = \sum_{n=0}^{\infty} p_n(t_i) \cos^2 \frac{1}{2} \Omega_{n+1} t_{\text{int}}, \quad (11)$$

and the outcome of a given measurement will yield (10a) or (10b) with probabilities  $p_a$  and  $1-p_a$ , respectively. [Comparison of Eqs. (10a) and (11) shows that  $\mathcal{N}_a = p_a = 1 - \mathcal{N}_b$ .] For each step of the iteration (atom  $i$ ), we thus proceed by computing  $p_a(t_i + t_{\text{int}})$  and numerically generate a random deviate  $0 \leq r \leq 1$ . If  $r > p_a$ , we say that the atom is measured to be in its excited state and the photon statistics are calculated according to Eq. (10a), otherwise the atom is found in its lower state and Eq. (10b) is used for the photon statistics. We can then introduce the effects of damping, Eq. (5), and proceed to the next iteration.<sup>7</sup>

The conditional choice of photon statistics (10a) or (10b), depending on the outcome of the measurement, is clear evidence of the back action of the measurement on the state of the cavity mode. Reference 7 discusses to which extent a “naive” interpretation of energy conservation is invalidated by such a procedure. We emphasize that although quantum mechanics is perfectly capable of computing the outcome of a *representative* sequence of measurements,<sup>8</sup> this procedure is not totally predictive, since there is an element of chance attached to it. It is highly unlikely that an experiment will reproduce exactly one of the sequences obtained numerically: Unless  $p_a$  is zero or unity, the measuring apparatus (field ionization) will produce a different sequence of random numbers than the computer, but of course, their average over a large number of realizations will be the same.

Sections III and IV illustrate two particularly simple examples of micromaser dynamics induced by the repeated measurements process. In both cases the cavity mode is initially assumed to be at thermal equilibrium and described by Eq. (6). The damping part of the micromaser evolution is treated by numerically integrating a truncated set of the coupled ordinary differential equations (5) over a time  $t_p \cong 1/R$  with initial condition (10a) or (10b). The truncation was checked by making sure that the numerical results were insensitive to further increase in the number of states. For these numerical studies, we parametrize the micromaser by the variables  $n_b, N_{\text{ex}}$ , and the pump parameter<sup>3</sup>

$$\Theta = \sqrt{N_{\text{ex}}} \kappa t_{\text{int}} / 2. \quad (12)$$

### III. QUANTUM DIFFUSION

The steady-state characteristics of the micromaser are presented in detail in Ref. 3. For large enough  $N_{\text{ex}}$ , the expectation value of the intracavity photon number  $\langle n \rangle$

undergoes a series of transitions as a function of the pump parameter  $\Theta$ . The first of these, at the gain = loss condition  $\Theta=1$ , corresponds to the conventional maser threshold and has the characteristics of a continuous phase transition. A succession of first-order-like phase transitions then follows in which the photon number increases abruptly for a small positive increment in  $\theta$ . In these regions the steady-state micromaser photon statistics is double peaked, with a strongly super-Poissonian character.

Reference 3 also introduces the semiheuristic Fokker-Planck equation for the probability  $p(\nu, \tau)$  of having  $n = \nu N_{\text{ex}}$  photons in the field at time  $t = \tau/\gamma$

$$\frac{\partial}{\partial \tau} p(\nu, \tau) = - \frac{\partial}{\partial \nu} [q(\nu) p(\nu, \tau)] + \frac{1}{2N_{\text{ex}}} \frac{\partial^2}{\partial \nu^2} [g(\nu, \tau) p(\nu, \tau)]. \quad (13)$$

Here  $n$  is treated approximately as a continuous variable,

$$q(\nu) \cong \sin^2(\sqrt{\nu}\Theta) - \nu \quad (14)$$

and

$$g(\nu) \cong \sin^2(\sqrt{\nu}\Theta) + \nu + 2\nu n_b. \quad (15)$$

This Fokker-Planck equation, and in particular the corresponding effective potential

$$V(\nu) = - \int d\nu \frac{q(\nu)}{g(\nu)}, \quad (16)$$

provide an intuitively appealing understanding of many of the characteristics of the micromaser, as discussed in detail in Ref. 3. For our present purposes, it is sufficient to note that the photon number distribution tends to accumulate near the global minimum of the effective potential  $V(\nu)$ , i.e., near one of the zeros  $\nu_0$  of the function  $q(\nu)$ . These zeros are the solutions of

$$\nu_0 = \sin^2(\sqrt{\nu_0}\Theta). \quad (17)$$

For  $\Theta < 1$  the (unique) minimum of  $V(\nu)$  is at  $\nu=0$ . At  $\Theta=1$  the minimum  $\nu_0=0$  turns into a local maximum and the mean photon number in the cavity starts to grow.

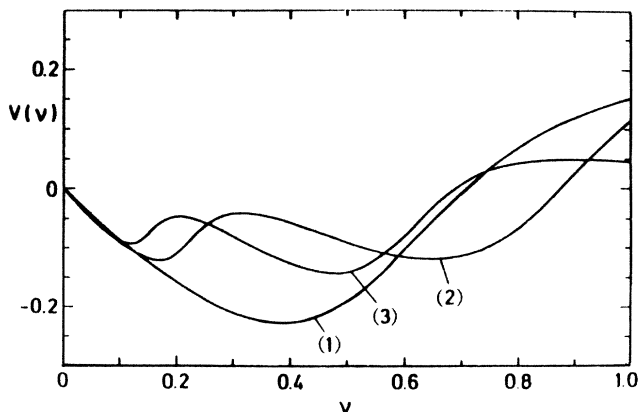


FIG. 1. Potential  $V(\nu)$ , where  $\nu = n/N_{\text{ex}}$ , for three values of the pump parameter (1)  $\Theta=4$ , (2)  $\Theta=2.116\pi$ , and (3)  $\Theta=8$ .

This is the maser threshold. As  $\Theta$  is further increased, the effective potential  $V(\nu)$  acquires an increasing number of minima. This is illustrated in Fig. 1, where  $V(\nu)$  is drawn for the three pump parameters  $\Theta=4$ ,  $2.116\pi$ , and  $8$ . The intermediate value of  $\Theta$  is precisely such that the global minimum at  $\nu=0.18$  is replaced by a global minimum at  $\nu=0.68$ . The micromaser exhibits a sharp jump in the intracavity mean photon number each time a minimum of  $V(\nu)$  loses its global character and is replaced in this role by the next one. In the vicinity of these transitions, the photon statistics are clearly double peaked.

These predictions, discussed in much more detail in Ref. 3, concern only ensemble averages. We now show how they can be improved upon by monitoring the state of the atoms as they exit the cavity. In particular, one would intuitively argue that as far as a single realization of the maser is concerned, the double-peaked photon statistics should be interpreted in terms of transitions between the two competing minima of the potential well due to quantum diffusion above the potential barrier. Repeated measurements on the system show that this is precisely what happens.

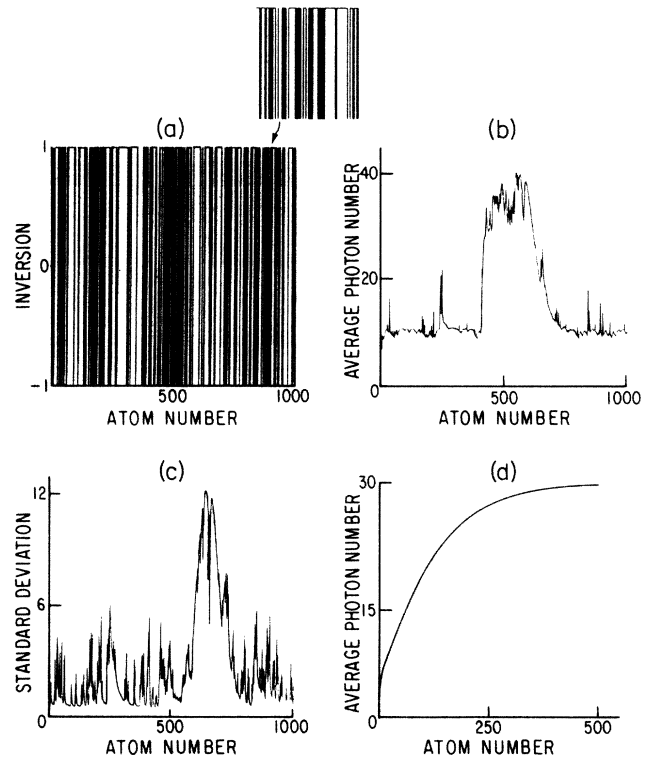


FIG. 2. (a) Raw data from repeated measurements of the states of two-level atoms exiting the micromaser cavity. The value “+1” corresponds to atoms measured in the upper state and “-1” to atoms measured in the lower state. The vertical lines are for visual help only; (b) average intracavity photon number  $\langle n \rangle$  and (c) standard deviation  $\sigma^2$  inferred from the raw measurements as a function of the number of atoms injected and measured; (d) conventional ensemble average  $\langle n \rangle$  for the same parameters  $N_{\text{ex}}=50$ ,  $\Theta=2.116\pi$ ,  $n_b=5$ . Figure 2(b) clearly shows diffusion between the minima of the effective potential.

Figure 2(a) gives the raw results of a typical sequence of measurements for the case (2) of Fig. 1, i.e.,  $N_{\text{ex}} = 50$ ,  $n_b = 5$ ,  $\Theta = 2.116\pi$ , for which  $n_l = 0.18N_{\text{ex}} = 9$  and  $n_u = 0.68N_{\text{ex}} = 34$ . They are labeled as  $+1$  or  $-1$  for the atom measured in the upper or lower state, respectively. The vertical lines are for visual help only. In contrast to the situation in real experiments, we assume for simplicity that all atoms exiting the resonator are detected in their state  $|a\rangle$  or  $|b\rangle$  with 100% quantum efficiency. For clarity, the inset of Fig. 2(a) shows the same results on an expanded horizontal scale. From this raw data and Eqs. (10), one can infer back the cavity mode photon statistics and mean photon number  $\langle n \rangle = \sum n p_n$ . This is precisely the strategy that would be followed in the laboratory to extract information on the intracavity field from the “clicks” at the detector(s).<sup>9</sup>

The results of this reconstruction are shown in Fig. 2(b), where diffusion between the two minima of the effective potential becomes quite clear. Note the good agreement between the numerical and effective potential predictions for  $n_l$  and  $n_u$ . Figure 2(c) gives the normalized standard deviation  $\sigma^2 = \langle (n - \langle n \rangle)^2 \rangle / \langle n \rangle$  of the photon statistics. It exhibits a broad peak during the slow down switching of  $\langle n \rangle$  from  $n_u$  to  $n_l$ . The upswitching, in contrast, is very fast and does not show any significant change in standard deviation in this example. For comparison, Fig. 2(d) gives the (ensemble-averaged) mean photon number  $\langle n(t) \rangle$  as obtained for the same parameters from the standard approach of Sec. II A. The difference between the two results is striking: In one case, one can truly follow the dynamics of the micromaser for all times, while the other only gives the transient approach to steady state.

#### IV. QUANTUM RELAXATION OSCILLATIONS

For a reservoir at zero temperature,  $n_b = 0$ , the steady-state photon statistics (7) reduces to

$$p_n = p_0 \frac{N_{\text{ex}}^n}{n!} \prod_{k=1}^n \sin^2(\theta \sqrt{k/N_{\text{ex}}}), \quad (18)$$

where  $p_0$  provides normalization and we have introduced the parameters  $N_{\text{ex}}$  and  $\Theta$ . A direct consequence of (18) is that for values of the pump parameter

$$\Theta = q\pi\sqrt{N_{\text{ex}}}, \quad q = 1, 2, 3, \dots, \quad (19)$$

the (ensemble average) steady state of the micromaser photon statistics is  $p_n = \delta_{n,0}$ , independent of the initial conditions. That is, the cavity field is in the vacuum state. This is because the vacuum field acts precisely as a  $2q\pi$  pulse for atoms spending time  $t_{\text{int}}$  inside the cavity, as readily seen by combining Eqs. (19) and (12) to give

$$\Theta / \sqrt{N_{\text{ex}}} = \kappa t_{\text{int}} / 2 = q\pi. \quad (20)$$

The vacuum state, as any number state, does not exhibit any intensity fluctuations and can act as a true  $2q\pi$  pulse. In most other cases, however, the inherent intensity fluctuations lead to the impossibility of achieving such a “perfect” interaction. This is the case, e.g., if the micromaser cavity has a finite temperature  $n_b \neq 0$ .

This situation is illustrated in Fig. 3. Here, condition (20) is fulfilled ( $N_{\text{ex}} = 5$ ,  $\Theta \cong 35$ ), but  $n_b = 10^{-3}$ . For the corresponding thermal initial field, the first atom experiences almost, but not exactly a  $10\pi$  pulse. Consequently the probability of measuring it in the upper state at the exit of the resonator is almost unity. Because the initial photon statistics is exceedingly narrow, there is almost exact conservation of the mean photon energy<sup>7</sup> and the resonator field remains practically unchanged. But as further atoms are injected, there is a small but finite probability that one of them will eventually be measured to exit in its ground state. This happens first in our example for atom  $\cong 310$ . In this case, the back-action on the cavity mode is particularly drastic: To a very good approximation, the average intracavity photon number is increased by one, and the field becomes almost, but not exactly, the number state  $|1\rangle$ .

For the parameters of this example, the probability for the next atom to exit in the upper state is about  $p_a \cong 0.98$ , see Fig. 3(b), so that it is also very likely for it to be measured in that state. This is precisely what happens in the subsequent measurements. Hence the cavity mode simply relaxes back at rate  $\gamma$  to a situation close to thermal equilibrium. As further atoms are injected, there is, however, a finite probability that eventually another atom will also exit in its lower state. In Fig. 3(b) this happens next for atom  $\cong 400$ . The same process then starts again, resulting in the dynamics of  $\langle n \rangle$  shown in Fig. 3(a). This is

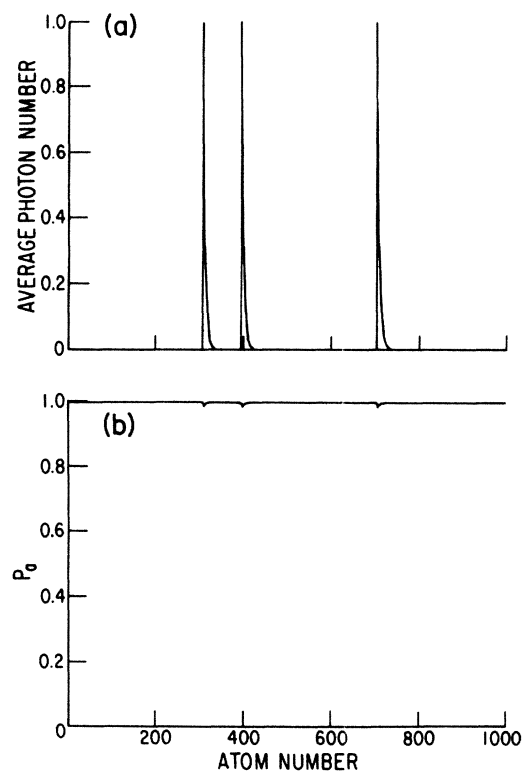


FIG. 3. (a) Inferred average photon number  $\langle n \rangle$  for  $N_{\text{ex}} = 5$ ,  $\Theta = 35$ ,  $n_b = 10^{-3}$  as a function of the number of atoms injected and measured; (b) probability for the corresponding atom to be measured in the upper state at it exits the cavity.

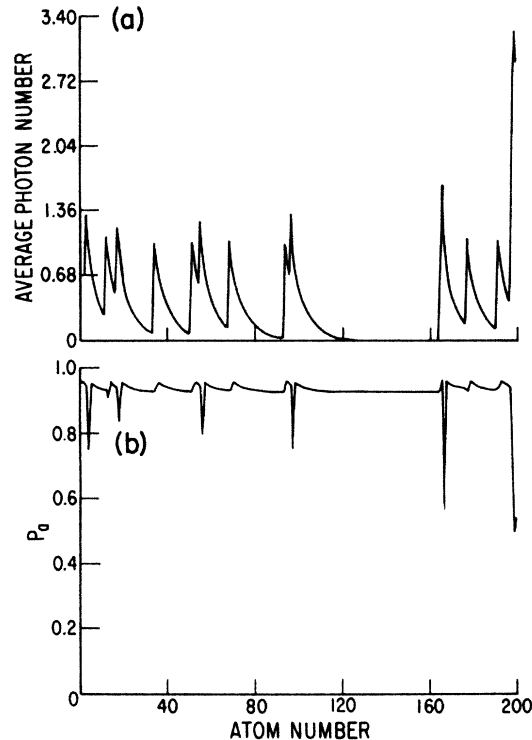


FIG. 4. Same as Fig. 3, but for  $N_{ex} = 5$ ,  $\Theta = 34.5$ ,  $n_b = 10^{-3}$ .

an example of quantum-measurement-induced relaxation oscillations.

Figure 4 shows a situation ( $\Theta = 34.5$ ,  $n_b = 10^{-3}$ ) where after an atom is measured to exit in the lower state, the probability  $p_a$  for the next one to exit in the upper state is significantly less than one [see Fig. 3(b)]. Under these conditions, the likelihood of measuring an atom to exit in the lower state during a cavity damping time is significant, leading to the dynamical behavior of  $\langle n \rangle$  shown in Fig. 4(a).

The measurement-induced dynamics of Fig. 4 resemble to some extent those of “period-2” classical motion. But there is no justification in drawing such an analogy: Every single measurement typically causes a strong back action on the state of the field, see Eqs. (10). At the same time, the probability  $p_a$  for an atom to exit in the upper state is very sensitive to both  $\kappa t_{int}$  and to the precise photon statistics (not just the average photon number) of the cavity mode. Hence the observed dynamics depend sensitively on the outcomes of all preceding measurements. Since every single measurement has an element of randomness attached to it, as described explicitly in Sec. II B, the dynamics are in final analysis governed by chance, in stark contrast to the classical case. The micromaser illustrates particularly clearly this irreconcilable difference between classical and quantum physics.<sup>1</sup>

## V. CONCLUSIONS

This paper shows how the results of repeated measurements on the exiting atoms can be used to extract dynamical information out of a micromaser. The observed dynamics are both measurement-induced and measurement-dependent. For instance, if we are content to verify only that the successive atoms exit the cavity, the micromaser reaches a unique steady state, in an ensemble average sense. In contrast, monitoring the state of the exiting atoms leads to complex dynamics, two cases of which have been illustrated.

These considerations carry beyond the specific example considered here. There is considerable present interest in the study of the quantum-classical interface in systems whose classical version exhibits dynamical instabilities such as period doubling or chaos.<sup>10</sup> In particular, for dissipative systems one is confronted with the apparent paradox that the quantum system density matrix typically evolves towards a unique steady state,<sup>11</sup> while the dynamical variables of its classical counterpart need not. In its conventional form quantum mechanics yields predictions for a large ensemble of identical systems, whereas classically the dynamics are interpreted in terms of single realizations. Even in the classical case, oscillations would not be evident on averaging over an ensemble unless the phase of the oscillations was fixed absolutely, which is not generically the case. We therefore claim that the paradox is only apparent. What should be considered is the quantum dynamics of a single representative system, which obviously is only apparent. What should be considered is the quantum dynamics of a single representative system, which obviously requires including the repeated measurements performed to monitor it.<sup>12</sup> We do not suggest that measuring the evolution of a quantum dynamical variable will make it behave in a classical fashion, but rather that in a single realization the dynamics of the system will become evident. In contrast to what is generally assumed in classical dynamics, the observed quantum “trajectories” are measurement induced and measurement dependent. Whether it is possible to obtain a classical or semiclassical behavior by performing an appropriate measurement on a quantum dynamical variable is a separate issue that goes beyond the scope of this paper.

## ACKNOWLEDGMENTS

We have benefited from numerous discussions with T. A. B. Kennedy, C. M. Savage, and H. Walther. Financial support from National Science Foundation Grant No. PHY-8603368 and from the Joint Services Optics Program is gratefully acknowledged. One of us (E.M.W.) is supported in part by an Air Force Weapons Laboratory Grant No. F29601-87-C-0052.

<sup>1</sup>W. E. Lamb, Jr., in *Chaotic Behavior in Quantum Systems, Theory and Applications*, edited by G. Casati (Plenum, New York, 1985), p. 353.

<sup>2</sup>D. Meschede, H. Walther, and G. Müller, *Phys. Rev. Lett.* **54**,

551 (1985).

<sup>3</sup>P. Filipowicz, J. Javanainen, and P. Meystre, *Phys. Rev. A* **34**, 3077 (1986).

<sup>4</sup>S. M. Barnett and P. L. Knight, *Phys. Rev. A* **33**, 2444 (1985).

<sup>5</sup>E. T. Jaynes and F. W. Cummings, Proc. IEEE **51**, 89 (1963).

<sup>6</sup>G. J. Milburn, Phys. Rev. A **36**, 744 (1987).

<sup>7</sup>P. Meystre, Opt. Lett. **12**, 669 (1987).

<sup>8</sup>For a closely related problem, see the recent on “quantum jumps” in (experiments): H. Demhelt, Bull. Am. Phys. Soc. **20**, 60 (1975); R. J. Cook and H. J. Kimble, Phys. Rev. Lett. **54**, 1023 (1985); W. Nagourey, J. Sandberg, and H. Demhelt, *ibid.* **56**, 2727 (1986); Th. Sauter, W. Neuhauser, P. Blatt, and P. E. Toschek, *ibid.* **57**, 1696 (1986); J. C. Bergquist, R. G. Hulet, W. M. Itano, and D. J. Wineland, *ibid.* **57**, 1699 (1986) and (theory): J. Javanainen, Phys. Rev. A **33**, 2121 (1986); A. Schenzle, R. G. DeVoe, and R. G. Brewer, *ibid.* **33**, 2127 (1986); C. Cohen-Tannoudji and J. Dalibard, Europhys. Lett. **1**, 441 (1986), P. Zoller, M. Marthe, and D. F. Walls, Phys. Rev. A **35**, 198 (1987).

<sup>9</sup>Recent micromaser experiments follow exactly this scheme and

use two successive field ionization detectors to detect atoms exiting both in the upper and lower state, H. Walther (private communication); see also J. Krause, M. O. Scully, and H. Walther, Phys. Rev. A **36**, 4547 (1987).

<sup>10</sup>For a discussion of chaos in a semiclassical version of the micromaser, see P. Meystre and E. M. Wright, in *Chaos, Noise and Fractals*, edited by E. R. Pike and L. A. Lugiato (Adam Hilger, Bristol, 1987), p. 102; T. A. B. Kennedy, P. Meystre, and E. M. Wright, in *Fundamentals of Quantum Optics II*, edited by F. Ehlotzky (Springer Verlag, Heidelberg and Berlin, 1987), p. 157.

<sup>11</sup>See, e.g., H. Haken, *Introduction to Synergetics* (Springer-Verlag, Heidelberg and Berlin, 1977).

<sup>12</sup>This is implicitly assumed in quantum jumps when considering multiple-time correlation functions.